NANO LETTERS

2007
Vol. 7, No. 3
547−551

Rectification of Ionic Current in a Nanofluidic Diode

Rohit Karnik,*,† Chuanhua Duan,† Kenneth Castelino,† Hirofumi Daiguji,‡ and Arun Majumdar†,§

Department of Mechanical Engineering, University of California, Berkeley, California 94720, Institute of Environmental Studies, Graduate School of Frontier Sciences, The University of Tokyo, Kashiwa, 277-8563, Japan, Department of Materials Science and Engineering, University of California, Berkeley, California 94720, and Materials Sciences Division, Lawrence Berkeley National Laboratory, Berkeley, California 94720

Received November 30, 2006; Revised Manuscript Received January 27, 2007

ABSTRACT

We demonstrate rectification of ionic transport in a nanofluidic diode fabricated by introducing a surface charge discontinuity in a nanofluidic channel. Device current–voltage (*I*–*V*) characteristics agree qualitatively with a one-dimensional model at moderate to high ionic concentrations. This study illustrates ionic flow control using surface charge patterning in nanofluidic channels under high bias voltages.

Nanofluidic channels with dimensions comparable to the Debye length exhibit unique transport characteristics due to effects of surface charge. Surface charge-governed ionic conductance,[1−3] diffusion,[4] pH-controlled protein transport,[5] and field-effect flow control[1,6] have been recently demonstrated in nanofluidic devices. Spatial change in the effect of surface charge along the length of a channel results in ionic concentration enhancement and depletion[7] and generation of space charge.[8] Similar effects occur when there is a spatial change in field effect inside a nanofluidic transistor.[1] This effect also gives rise to rectification of ionic current, which is a phenomenon well-known from its origins in semiconductor device physics. In nanofluidic systems, this occurs due to both asymmetric geometries and/or charge distributions. For example, in conical nanopores with uniform surface charge, asymmetric pore geometry results in rectification of ionic current that can mimic biological ion channels.[9−11] Bipolar membranes consisting of a cation-exchange membrane forming a junction with an anion-exchange membrane similarly exhibit current rectification[12,13] and find applications in production and recovery of acids and bases, chemical separations, and fuel cells.[14] However, these unique properties of transport in nanofluidic channels can be most effectively harnessed only through rational design and integration with other microfluidic and nanofluidic components, which is extremely difficult with current nanopore or bipolar membrane systems. Here, we directly pattern surface charge in nanofluidic channels to obtain a nanofluidic diode that exhibits ionic current rectification.

We have recently developed nanofluidic devices for field-effect flow control[1,6] and sensing[2] that are amenable to fabrication of networks of channels and integration with microfluidics, and the nanofluidic diode retains these. Daiguji et al. recently proposed and modeled a current-rectifying nanofluidic diode, consisting of opposite surface charges on either half of a nanofluidic channel.[15] Incorporation of such devices on a fluidic chip may find applications in control of ionic concentrations and pH, power generation from acidic and basic solutions, and could lead to new separation processes based on its unique transport properties. Further coupling surface chemical equilibria may result in as yet unexplored possibilities, as suggested by recent observations of current oscillations in nanopores.[16] While fabrication of a nanofluidic diode is challenging, herein we realize a nanofluidic diode using the newly developed method of diffusion-limited patterning[17] (DLP) to pattern the cationic protein avidin inside biotinylated nanofluidic channels (Figure 1). We demonstrate rectification of ionic current in the device and study ionic transport through the nanofluidic diode at various salt concentrations.

Nanofluidic channels 120 μm long, 4 μm wide, and ~30 nm in height were fabricated using a sacrificial polysilicon process described elsewhere.[1,2] The channel width was estimated from micrographs, and the channel height was

* Corresponding author. Current address: Department of Mechanical Engineering, Massachusetts Institute of Technology, Cambridge, Massachusetts 02139.

† Department of Mechanical Engineering, University of California, Berkeley.

‡ Institute of Environmental Studies, Graduate School of Frontier Sciences, The University of Tokyo.

§ Department of Materials Science and Engineering, University of California, Berkeley, and Materials Sciences Division, Lawrence Berkeley National Laboratory.

10.1021/nl062806o CCC: $37.00
Published on Web 02/21/2007

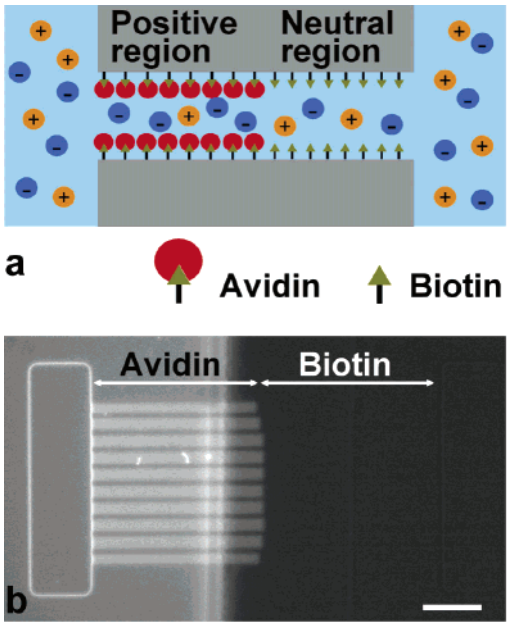

Figure 1. (a) Schematic diagram of a nanofluidic diode consisting of avidin patterned in half the channel. The other half has biotin moieties, which result in a close to neutral surface charge. (b) Epifluorescence image of the fabricated nanofluidic diode, showing fluorescently labeled avidin in half the channel. Scale bar 20 μm.

estimated from conductance measurements in 1 M KCl assuming a conductivity[18] of 11.13 Sm^{-1} (see Supporting Information). Figure 1 shows a set of ten parallel channels with an effective width of 40 μm. Two microfluidic channels were used to interface with the nanofluidic channels.

The channels were first modified with biotin and were characterized using conductance measurements (see Supporting Information). Biotin binds to the proteins avidin and streptavidin, with interactions being among the strongest noncovalent interactions known. To obtain asymmetric surface charge distribution, the method of diffusion-limited patterning[17] (DLP) was used. Briefly, 1 mg/mL solution of Alexa Fluor 488 labeled avidin (Invitrogen, Inc.) in 1× phosphate buffered saline (PBS) at pH 7.2 was introduced in only one of the microfluidic channels until half of the channels were covered with avidin (Figure 1b) (see Supporting Information). Because avidin is a highly cationic protein,[19−21] we expect a surface charge discontinuity in the nanofluidic channel. The diode was characterized using conductance measurements and current−voltage ($I-V$) curves were obtained (see Supporting Information). Finally, avidin was again introduced on both sides of the channels to obtain complete coverage of avidin, and the device was again characterized using conductance measurements. $I-V$ curves at low voltage bias (±50 mV) were linear and yielded information on surface charge characteristics and channel geometry, while those at high voltage bias (±10 V) exhibited current rectification.

To qualitatively explain rectifying behavior in our system, we use a one-dimensional model considering only electrophoretic and diffusive fluxes and the quasielectroneutrality condition. Local Donnan equilibrium[22] is assumed in order to relate ionic concentrations and potentials across the discontinuity in surface charge inside the channel and between the channel end and reservoir.

Consider a 1:1 electrolyte, and denote the cations and anions by n_+ and n_-, respectively. Further assume that the ions are nonreacting, and the (constant) fluxes of cations and anions along the channel are J_+ and J_-, respectively. For unit channel width, the mass conservation equations for each ionic species are

$$J_\pm = -hD\frac{dn_\pm}{dx} \mp h\mu n_\pm \nabla\varphi \tag{1}$$

D is ionic diffusivity, μ is ionic mobility, h is channel height, φ is electric potential, and x is the distance coordinate along the length of the channel. For a surface charge density of σ, the quasielectroneutrality condition gives

$$2\sigma/eh = n_- - n_+ \tag{2}$$

We use the Donnan equilibrium condition[22] to relate electric potentials and concentrations at the channel end and the reservoir as well as across the discontinuity in surface charge within the channel. Subscripts A and B refer to points on either side of the discontinuity.

$$\frac{n_{+A}}{n_{+B}} = \exp\left(\frac{e}{kT}(\varphi_B - \varphi_A)\right)$$
$$\frac{n_{-A}}{n_{-B}} = \exp\left(\frac{e}{kT}(\varphi_A - \varphi_B)\right) \tag{3}$$

Equation 1 was integrated analytically, and in conjunction with eqs 2−3, yielded a set of transcendental equations that was solved using Matlab (see Supporting Information). Ionic mobility was assumed to be 7.8×10^{-8} m^2/Vs for both K^+ and Cl^- ions.[18] Channel height and width were assumed to be 30 nm and 40 μm, respectively, and half of the total 120 μm length was assumed to be patterned with avidin.

The assumptions of one-dimensional transport, local Donnan equilibrium at the junctions, and electroneutrality are the major simplifying assumptions used in our model. Similar models were found to be sufficient to qualitatively explain rectification of transport in bipolar membranes[23] and nanopipettes[24] and do not significantly compromise the accuracy of results compared to the full Poisson−Nernst−Planck model of a nanofluidic diode, at least under forward bias[15] (see Supporting Information). Similarly, under reverse bias, the model yields concentration depletion and near-zero current, agreeing qualitatively with the full solution.[15] The one-dimensional assumption is reasonable because time for diffusion of ions across the channel is much smaller than transit time of the ions through the channel, and the ionic concentrations are reasonably described by a uniform potential across the channel (see Supporting Information). The assumption of local Donnan equilibrium has been justified in the case of a bipolar membrane.[23] The assumption fails if the potential drop due to ionic current between two points is comparable to the potential difference between those

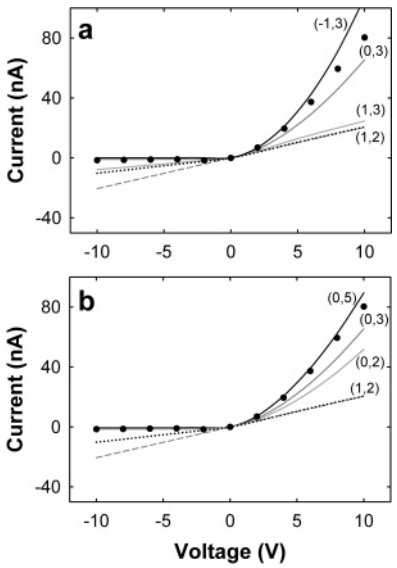

Figure 2. Diode $I-V$ characteristics at 10 mM KCl. Solid circles represent experimental data, while the dashed line has slope equal to the conductance measured using a voltage bias range of −50 to 50 mV. Solid lines are theoretical predictions for a 120 μm long, 40 μm wide channel with a height of 30 nm and a surface charge of 1, 0, and −1 mC/m^2 in the biotin half of the channel and 3 mC/m^2 in the avidin half of the channel (a), and a surface charge of 0 mC/m^2 in biotin half the channel and 2, 3, and 5 mC/m^2 in the avidin half of the channel (b). Theoretical predictions for experimentally measured surface charges (see Supporting Information) of 1 mC/m^2 on the biotin half and 2 mC/m^2 on the avidin half (dotted lines) exhibit current decrease under reverse bias, but no significant current enhancement under forward bias in (a) and (b). Biotin side is at a higher potential under forward bias.

two points. Under forward bias, there is no depletion region at the junction, and the potential drop is small compared to the applied voltage bias. Under reverse bias, there is almost zero ionic current, and the potential drop due to ionic current is small compared to the potential drop across the depletion region that forms at the junction.[15] Moreover, this current being close to zero does not affect our subsequent arguments or comparison with experimental results. Our model and full solutions of the Poisson−Nernst−Planck equations[15] suggest that a depletion region does not form in the channel if the surface charge changes in (nonzero) magnitude across a junction but not in sign. We have incorporated here the simplest possible model that gives some intuition and succeeds in qualitatively explaining the current rectification phenomenon.

Experimental and theoretical $I-V$ curves obtained at KCl concentration of 10 mM in ±10 V bias range show rectification of ionic current (Figure 2). $I-V$ curves obtained in the ±50 mV bias range were linear. Experimental data are denoted by dark circles, while the dashed lines have slopes equal to conductance measured in the low bias regime (±50 mV). Relative to current extrapolated linearly from low-bias measurements, there is current enhancement when the biotin side is at a positive potential (forward bias) and current depletion under reverse bias. Theoretical predictions (solid lines) show qualitative agreement with experimental results. Figure 2a shows theoretical predictions with a surface charge of 3 mC/m^2 on the avidin side and −1, 0, and 1 mC/m^2 on the biotin side. Current rectification occurs even when the surface charge on either half is of the same sign; however, rectification is enhanced when one-half of the channel has no charge or charge of the opposite sign. Figure 2b shows theoretical predictions with a surface charge of 2, 3, and 5 mC/m^2 on the avidin side and 0 mC/m^2 on the biotin side. As the surface charge on the avidin side increases, current enhancement increases. It is also worth noting that the direction of current enhancement is consistent with a higher surface charge on the avidin side ($\sigma_{avidin} - \sigma_{biotin} > 0$), which is expected due to the highly cationic nature of avidin.

Comparison of experimental data with theoretical predictions suggests that the charge on the biotinylated side is close to neutral or negative. However, conductance measurements of the biotinylated channels before patterning avidin and of the fully avidin-coated channels indicate that the magnitude of surface charge of the avidin-coated surface is approximately 2 mC/m^2, while that of the biotinylated surface is approximately 1 mC/m^2. Experiments on another device showed that surface charge was positive for both avidin-coated and biotinylated surfaces (see Supporting Information). For surface charges of 2 mC/m^2 on the avidin side and 1 mC/m^2 on the biotin side, our model predicts mild current rectification, with some current depletion under reverse bias but almost no current enhancement under forward bias (Figure 2). This is in contrast to the observed current enhancement under forward bias and marked current depletion under reverse bias. The assumptions of the one-dimensional model have been examined by comparison with the full solution of the Poisson−Nernst−Planck equations,[15] and it has been found to be valid at least in the forward bias case. It makes it unlikely that the one-dimensional transport assumption or the Donnan local equilibrium assumption can account for the discrepancy in surface charge. The most likely reason for the observed discrepancy is that surface properties being difficult to control, surface charge may have changed in the avidin patterning step or in the final step of coating the entire surface with avidin. Conductance measurements (see Supporting Information, Figure S1) reveal that, while diode conductance lies in between those of the biotinylated channel and the fully avidin coated channels, its conductance deviates by approximately 50% from the expected value calculated using conductance of the biotinylated and avidin-coated channels. It may also indicate that characterization of transport in such systems based only on surface charge is inadequate. It must be noted that modeling of current rectification in bipolar membranes[13,22,23] and nanopores[25] shows that quantitative prediction of transport in such systems is difficult and only qualitative agreement may be expected.

To gain some insight into the mechanism of current rectification, ionic concentration profiles and corresponding electric potential predicted theoretically are shown for 10 mM KCl at bias voltages of +5 and −5 V, respectively (Figure 3). The left half of the channel is assumed to have a surface charge of 3 mC/m^2 (avidin-coated), while the right half is assumed to be neutral (biotinylated). When there is

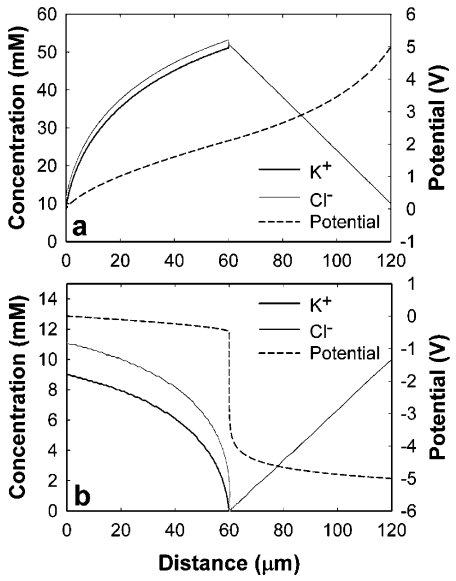

Figure 3. Theoretical predictions of the ionic concentration and electric potential profiles along nanofluidic diode calculated using the one-dimensional model. The avidin half of the channel has a positive charge of 3 mC/m^2, and the biotin half is neutral. (a) Under forward bias of 5 V, there is concentration enhancement in the channel. (b) Under a reverse bias of −5 V, there is concentration depletion in the channel, and the electric potential drops sharply at the junction of positive and neutral surface charge. Channel height is 30 nm, and KCl concentration is 10 mM.

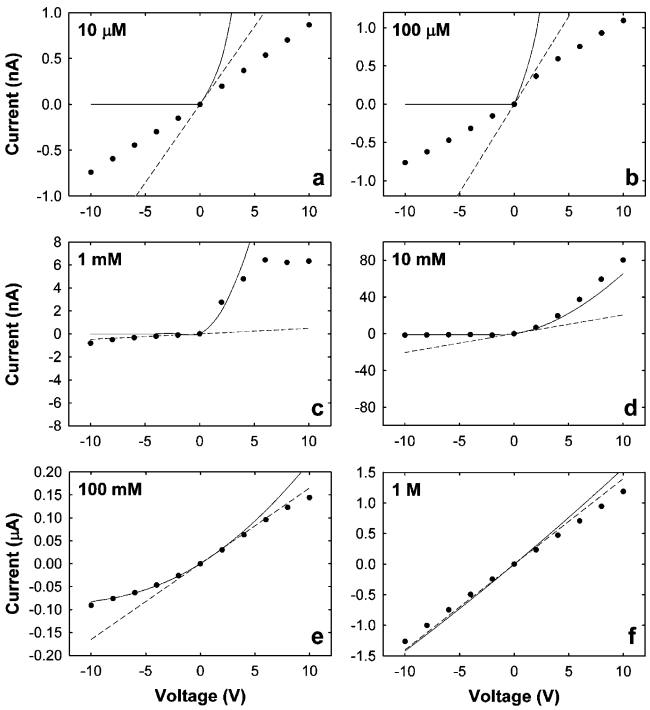

Figure 4. Diode $I-V$ characteristics at different KCl concentrations (a−f). Solid circles represent experimental data, while the dashed line has slope equal to the conductance measured using a voltage bias range of −50 to 50 mV. Solid lines are theoretical predictions for a 120 μm long, 40 μm wide channel with a height of 30 nm and a surface charge of 3 mC/m^2 in the avidin half of the channel and 0 mC/m^2 in the biotin half of the channel. Biotin side is at a higher potential under forward bias.

no electric field along the channel, negative chloride ions accumulate in excess in the avidin half of the channel to neutralize the positive charge on avidin. When a positive voltage bias is applied to the biotin side, chloride ions from the avidin side travel to the biotin side. It results in concentration enhancement in the channel, and the magnitude of the axial electric field varies accordingly such that a constant current of chloride ions is maintained. The electric potential varies smoothly along the channel, there is high ionic current, and the diode is in forward bias. However, when the biotin side is at a negative voltage bias, chloride counterions in the avidin side are driven away from the biotin side. It results in concentration depletion inside the channel, and the electric potential drops sharply across the avidin−biotin junction. Under this condition, very little ionic current flows through the channel, and the diode is in reverse bias. This mechanism is similar to that of current rectification in conical nanopores and bipolar membranes, in that current enhancement is associated with concentration enhancement and current depletion is associated with concentration depletion.

Diode characteristics for different KCl concentrations are shown in Figure 4, along with theoretical predictions for a surface charge of 3 mC/m^2 on the avidin side and 0 mC/m^2 on the biotin side. Theoretical $I-V$ curves are used with the intention of qualitatively illustrating general trends predicted by the model. It is seen that current rectification is prominent at intermediate concentrations of 1 mM and 10 mM KCl, but not at higher or lower concentrations. At higher concentrations of KCl, the effect of surface charge is small due to high bulk ionic concentration ($\sigma/eh < n_{bulk}$). At 1 M KCl, surface charge effects are negligible and the theoretical and experimental $I-V$ curves exhibit linear characteristics. The effect of surface charge is evident at 100 mM KCl. Theory predicts a slight current rectification at 100 mM KCl, which is also observed experimentally, although current enhancement is not seen.

While the experimental results match closely with theoretical predictions at KCl concentrations of 1 mM and above, there is a large deviation at lower KCl concentrations of 10 and 100 μM. Surprisingly, experimental data show current decrease under forward bias instead of the expected current enhancement and do not exhibit the expected current depletion under reverse bias. In addition, current saturation observed at 1 mM under forward bias is not expected from theoretical predictions. There are several factors that affect ionic transport and complicate the system at lower KCl concentrations that could account for high current under reverse bias. Enhanced water dissociation in bipolar membranes results in a large current under reverse bias,[22,26] which may also be expected to occur in our device and may explain the high current under reverse bias. This water dissociation could also lead to pH changes resulting in variation of surface charge on the biotinylated surface, which could further increase the current. However, under forward bias, concentration polarization effects arising near the channel entrance[27] may play a role in the observed current decrease (see Supporting Information). Solution of the full Poisson−Nernst−Planck equations in the case of a nanofluidic diode

exhibits a significant potential drop and concentration depletion in the reservoir,[15] which may decrease the ionic current. These results point to the importance of the microfluidic−nanofluidic interface, which is poorly understood and difficult to model. It is clear from the above discussion that, while rectification can be qualitatively explained, a complete understanding of ion transport in the nanofluidic diode will require further study. However, there is clear evidence for rectification of ionic transport at higher KCl concentrations, which agrees qualitatively with theoretical predictions of the one-dimensional model.

In this work, we have demonstrated a current-rectifying nanofluidic diode using the method of diffusion-limited patterning. Device $I-V$ characteristics agree qualitatively with a one-dimensional theoretical model at moderate to high ionic concentrations. At low ionic concentrations, $I-V$ characteristics suggest that effects at the channel entrance and water dissociation play a significant role in transport through the diode. This study illustrates flow control using surface charge patterning in nanofluidic channels in the regime of high voltage bias. This device can be rationally designed and is amenable to integration with other nanofluidic and microfluidic channels. Our experiments suggest that the nanofluidic diode or devices based on similar principles could find applications in control of pH and ionic concentrations and separation processes.

Acknowledgment. We thank Peidong Yang and his group (UC Berkeley) for continued collaboration in nanofluidics. This work was supported by Basic Energy Sciences, Department of Energy, as well as the National Science Foundation. Devices were fabricated at the Microfabrication Laboratory at the University of California, Berkeley.

Supporting Information Available: Materials and methods, one-dimensional model for ion transport in a nanofluidic diode, validity of the uniform potential assumption, conductance measurement at low bias, and limiting current at the entrance of a nanofluidic channel. This material is available free of charge via the Internet at http://pubs.acs.org.

References

(1) Karnik, R.; Fan, R.; Yue, M.; Li, D. Y.; Yang, P. D.; Majumdar, A. *Nano Lett.* **2005**, *5*, 943−948.
(2) Karnik, R.; Castelino, K.; Fan, R.; Yang, P.; Majumdar, A. *Nano Lett.* **2005**, *5*, 1638−1642.
(3) Stein, D.; Kruithof, M.; Dekker, C. *Phys. Rev. Lett.* **2004**, *93*, 035901.
(4) Plecis, A.; Schoch, R. B.; Renaud, P. *Nano Lett.* **2005**, *5*, 1147−1155.
(5) Schoch, R. B.; Bertsch, A.; Renaud, P. *Nano Lett.* **2006**, *6*, 543−547.
(6) Karnik, R.; Castelino, K.; Majumdar, A. *Appl. Phys. Lett.* **2006**, *88*, 123114.
(7) Pu, Q.; Yun, J.; Temkin, H.; Liu, S. *Nano Lett.* **2004**, *4*, 1099−1103.
(8) Wang, Y. C.; Stevens, A. L.; Han, J. Y. *Anal. Chem.* **2005**, *77*, 4293−4299.
(9) Siwy, Z.; Fulinski, A. *Phys. Rev. Lett.* **2002**, *89*, 198103.
(10) Siwy, Z.; Apel, P.; Baur, D.; Dobrev, D. D.; Korchev, Y. E.; Neumann, R.; Spohr, R.; Trautmann, C.; Voss, K. O. *Surf. Sci.* **2003**, *532*, 1061−1066.
(11) Siwy, Z.; Heins, E.; Harrell, C. C.; Kohli, P.; Martin, C. R. *J. Am. Chem. Soc.* **2004**, *126*, 10850−10851.
(12) Lovrecek, B.; Despic, A.; Bockris, J. O. M. *J. Phys. Chem.* **1959**, *63*, 750−751.
(13) Hurwitz, H. D.; Dibiani, R. *J. Membr. Sci.* **2004**, *228*, 17−43.
(14) Xu, T. W. *Desalination* **2001**, *140*, 247−258.
(15) Daiguji, H.; Oka, Y.; Shirono, K. *Nano Lett.* **2005**, *5*, 2274−2280.
(16) Siwy, Z. S.; Powell, M. R.; Petrov, A.; Kalman, E.; Trautmann, C.; Eisenberg, R. S. *Nano Lett.* **2006**, *6*, 1729−1734.
(17) Karnik, R.; Castelino, K.; Duan, C.; Majumdar, A. *Nano Lett.* **2006**, *6*, 1735−1740.
(18) Lide, D. *Handbook of Chemistry and Physics*, 73rd ed.; CRC Press, Boca Raton, FL, 1992.
(19) Donovan, J. W.; Ross, K. D. *Biochemistry* **1973**, *12*, 512−517.
(20) Green, N. M. *Methods Enzymol.* **1990**, *184*, 51−67.
(21) Delange, R. J.; Huang, T. S. *J. Biol. Chem.* **1971**, *246*, 698−709.
(22) Bassignana, I. C.; Reiss, H. *J. Membr. Sci.* **1983**, *15*, 27−41.
(23) Ohki, S. *J. Phys. Soc. Jpn.* **1965**, *20*, 1674−1685.
(24) Wei, C.; Bard, A. J.; Feldberg, S. W. *Anal. Chem.* **1997**, *69*, 4627−4633.
(25) Fulinski, A.; Kosinska, I.; Siwy, Z. *N. J. Phys.* **2005**, *7*, 132.
(26) Ramirez, P.; Rapp, H. J.; Mafe, S.; Bauer, B. *J. Electroanal. Chem.* **1994**, *375*, 101−108.
(27) Bassignana, I. C.; Reiss, H. *J. Phys. Chem.* **1983**, *87*, 136−149.

NL062806O